



RUTGERS

School of Environmental
and Biological Sciences

BIOAEROSOL RESEARCH AND TECHNOLOGY

Evaluation of the SKC PPI Impactor Performance

Project Report

Principal Investigator:
(Contact)

Gediminas Mainelis, Ph.D.
Professor
Department of Environmental Sciences
Rutgers, The State University of New Jersey
14 College Farm Road
New Brunswick, New Jersey 08901-8551
Phone: 848-932-5712
Fax: 732-932-8644
Email: mainelis@envsci.rutgers.edu

Principal Investigator:

Taewon T. Han, Ph.D.
Assistant Research Professor
Department of Environmental Sciences
Rutgers, The State University of New Jersey.
Email: han@envsci.rutgers.edu

PI's Signature and Date _____



Objective

The goal of this project was to evaluate the performance of respirable SKC PPI impactors, namely the disposable models operating at 2 and 4 L/min (referred to as 2-L/min-PPI and 4-L/min-PPI in the report, respectively) and also reusable models operating at 2 and 4 L/min (referred to as 2- L/min-Re-PPI and 4- L/min-Re-PPI). The PPI impactors have been designed to follow ISO 7708/CEN criteria for respirable particles. The following impactor performance parameters were determined:

- a) Penetration efficiency as a function of aerodynamic particle diameter when challenged with polydisperse and monodisperse aerosol particles.
- b) Cut-off size (d_{50}) when challenged with polydisperse and monodisperse aerosol particles.
- c) Bias map for the investigated samplers.

Methods

Test Particles

The performance of the SKC PPI impactors was investigated:

- a) Experimentally, with polydisperse NaCl particles, which were produced by aerosolizing liquid NaCl suspension. The aerodynamic diameter of the aerosolized NaCl was determined using an Aerodynamic Particle Sizer (APS) (TSI, Inc., Shoreview, MN).
- b) Experimentally, with monodisperse polystyrene latex (PSL) particles of the following nominal sizes: 1.1, 2.9, 4.8 μm .
- c) Theoretically, through the use of bias maps for all PPI models when aerosol distributions with different mass median diameters (MMAD) and geometric standard deviations (GSD) are used as challenge particles, and the collected mass concentration is calculated based on the experimental penetration efficiency data obtained through earlier steps.

Tested Samplers

For each step above, two PPI impactors designed to operate at 2 L/min (SKC PN 225-385), two PPI impactors designed to operate at 4 L/min (SKC PN 225-387), one reusable PPI impactor designed to operate at 2 L/min (SKC PN 225-380), and one reusable PPI impactor designed to operate at 4 L/min (SKC PN 224-382) were investigated. A total of six PPI impactors were tested.

Once the six PPI impactors were investigated, the following additional experiments were performed:

- Evaluation of the penetration efficiency of 4-L/min-Re-PPI at its nominal flow rate of 4.0 L/min and 4.3 and 4.5 L/min to investigate how the increased flowrate affects the sampler's performance.
- Evaluation of the penetration efficiency of 4-L/min-PPI when the impactor was operating facing down and sideways relative to the airflow.



Experimental setup

The impactors were evaluated using the experimental setup shown in Picture. 1. The investigators have used such and similar setups in other studies. Here, test particles were aerosolized using a Collison nebulizer operated at 2.5 L/min and 20 psi pressure. The produced aerosol was diluted with a HEPA-filtered air at a flow rate of 20 L/min. This resulting aerosol passed through a charge neutralizer Po-210, and the neutralized aerosol stream was diluted further with a HEPA-filtered airflow of 32-85 L/min depending on the PPI model to be tested. (The airflow was adjusted to achieve isokinetic sampling conditions for the reference probe in the test section). The final aerosol stream entered a mixing box, from where it was directed downward. First, the stream passed through two static blenders and a honeycomb section to mix and laminarize the flow. The laminar flow (Reynolds number = 380-750) then entered the test section of 7.75 inches in inner diameter. In the test section, we positioned a PPI impactor to be tested and a reference probe side-by-side. From the PPI impactor and the probe, vertical sampling lines extended downward and were connected to the Aerodynamic Particle Sizer (TSI, Inc.) (APS). Using switches to direct an aerosol stream from each line to the APS, we alternately measured the size distribution of aerosol that penetrated the PPI and size distribution of aerosol that was sampled by the reference probe, i.e., reference aerosol. The uncollected particles exited the test system through an open-ended tube into an operating biosafety cabinet where they were removed from the airflow by filtration.

Sampling adapter and reference probe

The PPI impactors were tested with the filtration section removed, and, therefore, adapters were needed to secure the impaction section to the PPIs to the sampling line. In addition, reference probes were needed to sample the test aerosol in the test section at isokinetic conditions. Therefore, we designed and 3D-printed a unique structure that served as both the adapter for the PPI and an isokinetic sharp-edged probe. Such adapters (Picture 2) were prepared for both the disposable and reusable PPI impactors. The adapter for the Re-PPI has a “lip” to accommodate the Re-PPI structure, but its inner diameter is the same as that of the adapter for the disposable PPI. The adapters for the Re-PPI have “ears” to accommodate screws to secure airtight connection of the samplers to the probes. The adapters were coated with copper-based conductive spray to minimize any static effects during sampling. Since identical adapters are used for the impactor and for reference sampling, any transmission losses between the two are the same, and that allows for accurate determination of the PPI penetration efficiency without a need for additional corrections.

Measurement procedure

The air velocity in the test section was set to 0.06 m/s when testing 4-L/min-PPIs and 0.03 m/s when testing 2-L/min-PPIs. The air velocity across the test chamber varied within 5%. Once the particle aerosolization started, the aerosol was allowed to equilibrate for 5-10 minutes to achieve a stable aerosol concentration in the test section as measured by the APS. Once the concentration was stable, we alternatively measured particle concentration leaving the impactor (C_{PPI}) and particle concentration sampled by the reference probe (C_{ISO}). Seven such interspersed measurements were performed (4 with the reference and 3 with the impactor), and they constituted one set of measurements. For each test impactor and each test particle type, three sets were

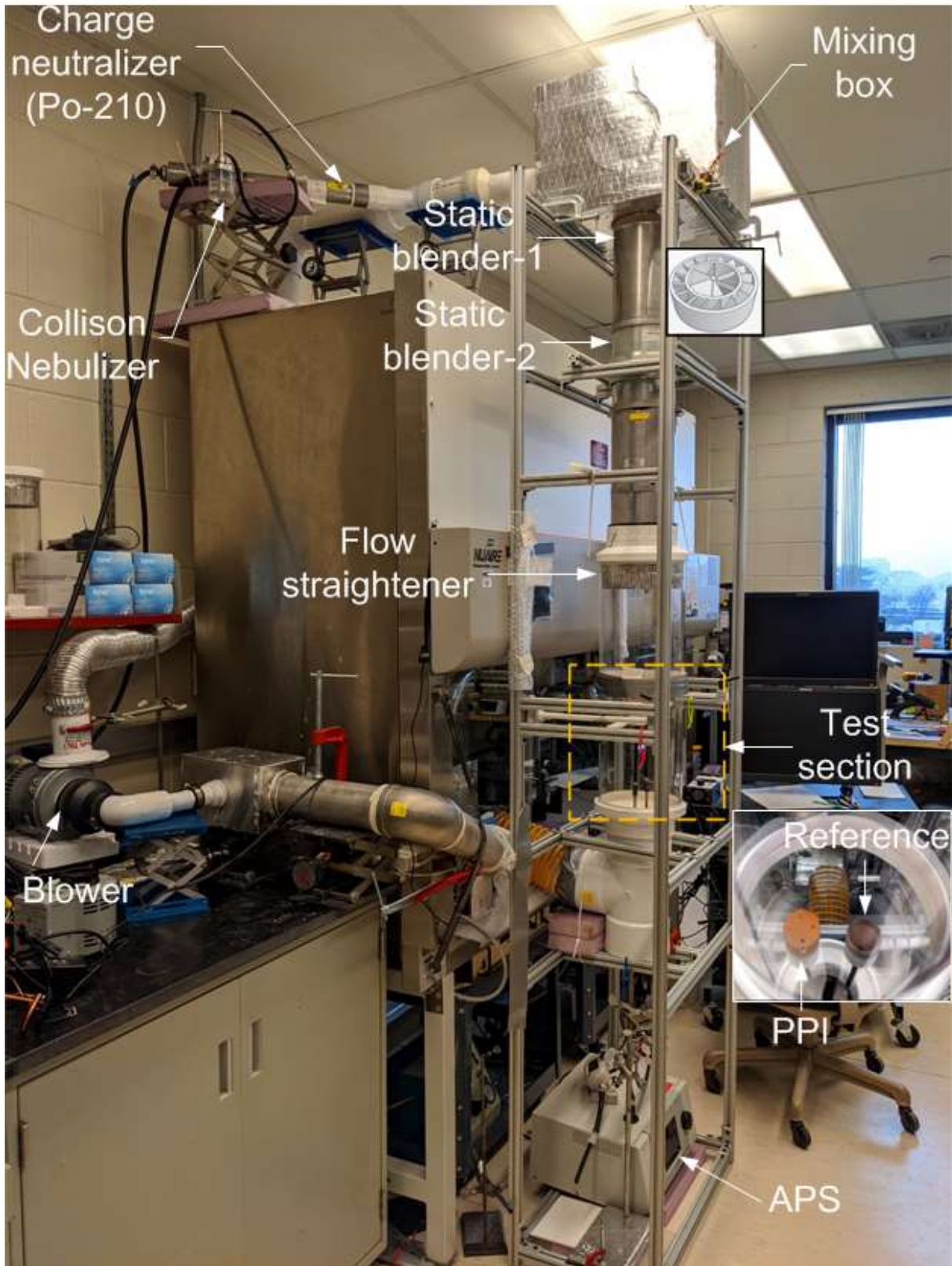


performed with a PPI impactor situated to the left of the probe and three sets with the same impactor situated to the right of the probe. We alternated impactor positions to account for any particle distribution variation inside the test section.

The penetration efficiency of each PPI impactor was determined by comparing C_{ISO} and C_{PPI} :

$$Penetration = C_{PPI}/C_{ISO} \quad (1)$$

The data presented below show the penetration efficiency of individual tests and then the average penetration efficiency for NaCl particles and PSL particles. The average data obtained with NaCl particles and PSL particles were fitted with a 3 parameter sigmoid regression function, and the resulting penetration functions and the cut-off sizes (d_{50}) are presented for each impactor type.



Picture 1. The test setup used to evaluate PPI impactors.



(a)



(b)



(c)



(d)

Picture 2. Adapters that were used to test PPI impactors. a) Adapter for disposable PPI; it also serves as an isokinetic probe. b) and c) Adapter for Re-PPI. d) Re-PPI coupled with an adapter.



Bias Map

Once the particle penetration data for each PPI model was determined, a bias map for each PPI model, as well as for each additional test was calculated. The bias map shows the difference, or bias, Δ , between a mass concentration captured by the tested device, C , relative to the mass concentration C_R that would be captured by a reference device when both a challenged with the same aerosol (1):

$$\Delta \equiv \frac{C - C_R}{C_R} \quad (2)$$

The reference device, in our case, was the ideal respirable sampling convention. The bias map was generated for different hypothetical aerosols ranging in MMAD (mass median aerodynamic diameter) from 1 to 25 μm and having different size dispersions in terms of GSD (geometric standard deviation) that range from 1.75 to 3.5. However, biases for distributions beyond the line of MMAD = 10 μm and GSD = 1.5 and MMSD = 25 μm and GSD = 2.75 are not shown as they rarely occur (1). For the same reason, biases for MMAD = 1 μm and with GSD ranging from 2.25 to 3.5 are also not included.

Using data from all data points, we also calculated an average bias for each sampler of the test condition. The presented bias maps and color codes within the maps indicate how much a PPI oversamples or undersamples the aerosol compared to an ideal respirable sampler when challenged with different aerosols.



Results

Six different SKC PPI units were tested:

- 2-L/min-PPI (#38334 and #38349)
- 4-L/min-PPI (#03582 and #03583)
- 2-L/min-Re-PPI (Re-PPI)
- 4-L/min-PPI (Re-PPI)

The cut-off sizes of the tested samplers are summarized in Table 1, and the penetration characteristics of individual impactors, as well as their bias maps, are shown in Figures 1-6. Reusable impactor operated at 4 L/min showed a d_{50} of 4.27 μm , and therefore, the second set of measurements was performed with this impactor. The data (Fig. 7) confirmed the first measurement. Therefore, two additional sets of measurements were performed with this impactor at an operating flowrate of 4.3, and 4.35 L/min, and those data are shown in Figures 8 and 9. All data for the Re-PPI 4 L/min are presented in Figure 10. The penetration efficiency of 4-L/min-PPI (#03582) when facing downward and to the side, as well as corresponding bias maps, are presented in Figs. 11 and 12, respectively.

Table 1. The summary of d_{50} cut sizes.

Sodium chloride particles				PSL particles			
d_{50} cut size, μm				d_{50} cut size, μm			
PPI	#38334	#38349	AVG	PPI	#38334	#38349	AVG
2 LPM	3.97	3.92	3.95	2 LPM	4.00	3.95	3.98
PPI	#03582	#03583	AVG	PPI	#03582	#03583	AVG
4 LPM	3.97	4.04	4.01	4 LPM	3.96	4.08	4.02
Re-PPI				Re-PPI			
2 LPM	4.07			2 LPM	4.08		
Re-PPI	1 st test	2 nd test		Re-PPI			
4 LPM	4.27	4.27		4 LPM	4.28		

Cut size (d_{50}) of RePPI-4 L/min at different flow rates when tested with NaCl particles, μm

Re-PPI	
4.3 L/min	3.96
Re-PPI	
4.5 L/min	3.83



Table 1. The summary of d_{50} cut sizes (continued).

Cut size (d_{50}) of 4-L/min-PPI (#03582) at
different orientations when tested with
NaCl particles, μm

Facing downward	4.04
Facing sideways	4.04



(a)

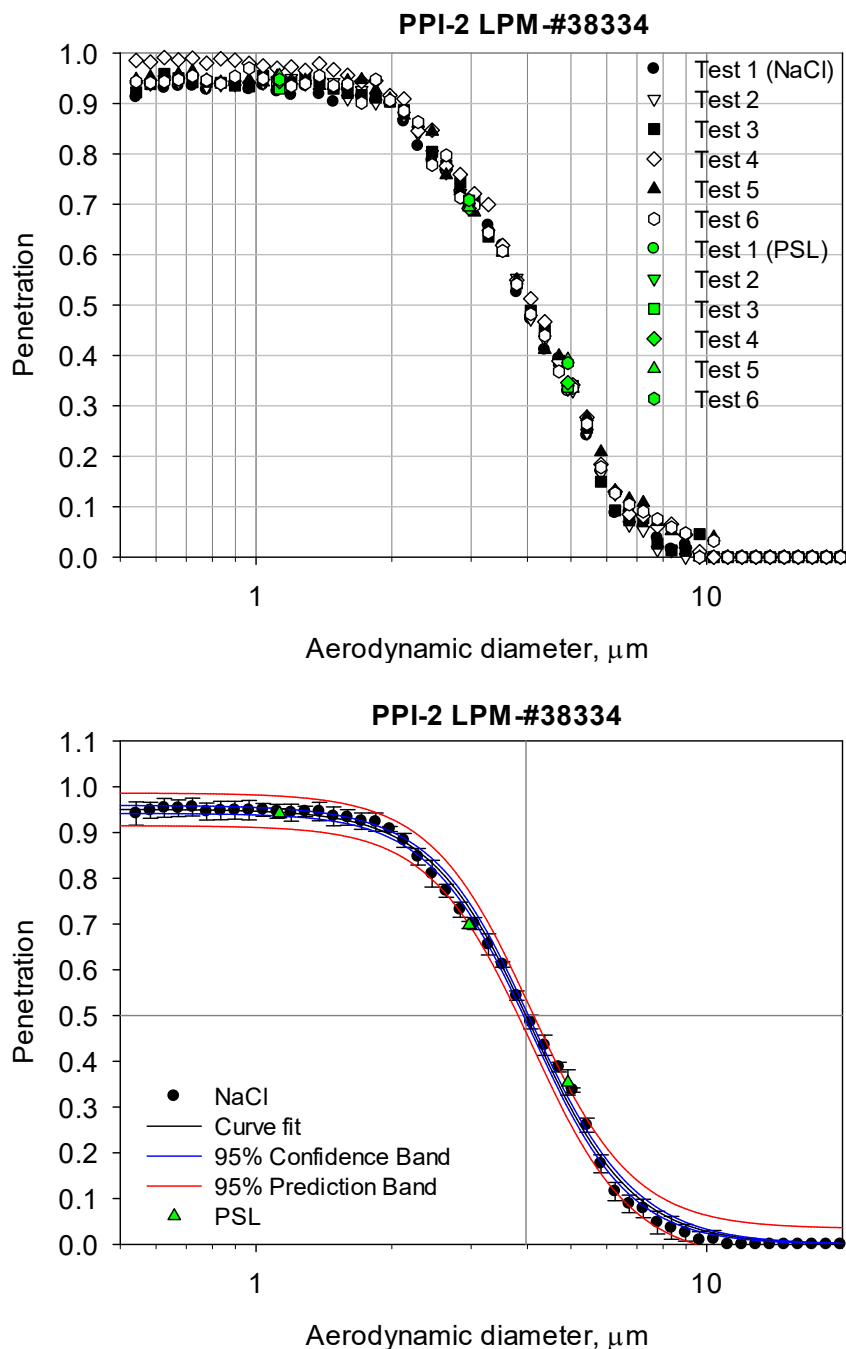


Figure 1. SKC 2-L/min-PPI-2 impactor penetration curve as a function of particle size: a) individual data points and b) average values and standard deviations for each particle size and type based on six tests.

The data were fitted with a 3 parameter sigmoid regression equation resulting in the following equation:

$$\text{with NaCl: } \eta = \frac{0.9506}{1 + \left(\frac{dp}{4.078}\right)^{3.873}} \quad R^2=0.9983 \quad \text{with PSL: } \eta = \frac{0.9613}{1 + \left(\frac{dp}{4.109}\right)^{3.004}} \quad R^2=1 \quad (1)$$

Based on the fit, the d_{50} cut size (aerodynamic particle size at which 50% penetration occurs) of the impactor was 3.97 μm with NaCl and 4.0 μm with PSL at the operating flow rate of 2 L/min.

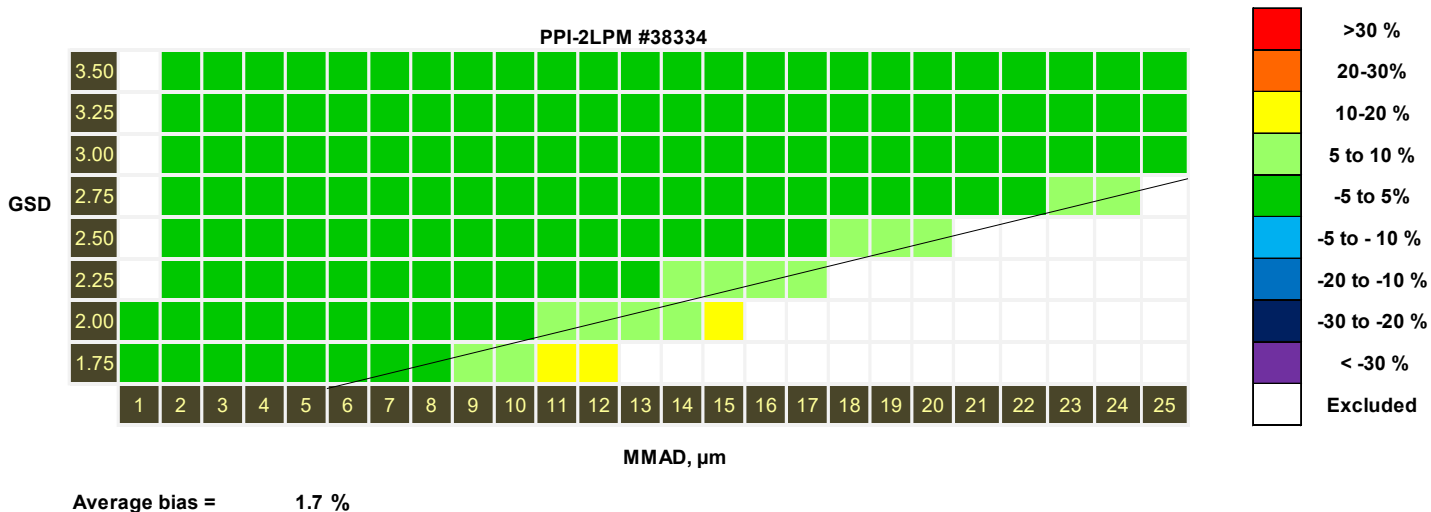
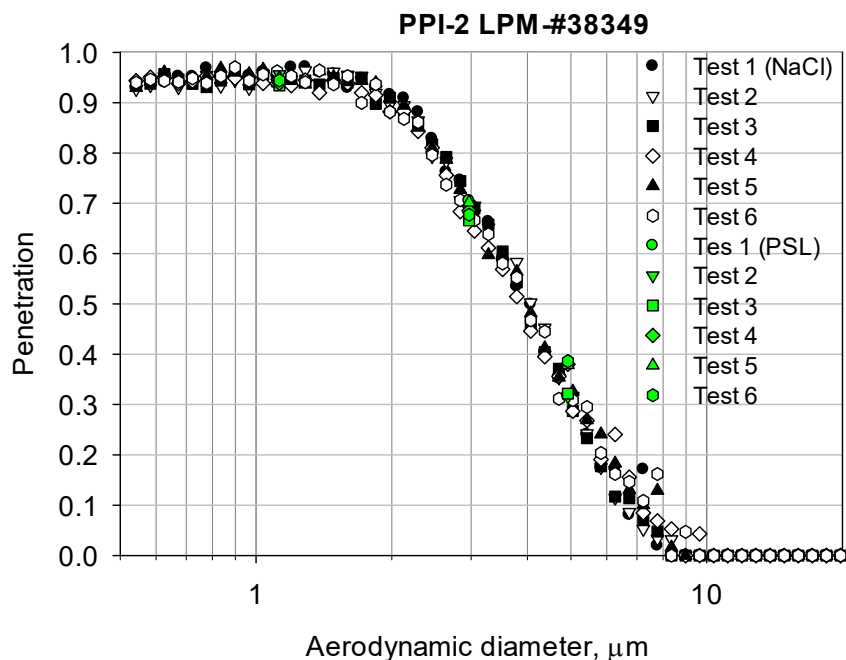


Figure 1c. Bias map for the SKC 2-L/min-PPI impactor (#38334) for different particle size distributions (MMAD and GSD).



(b)

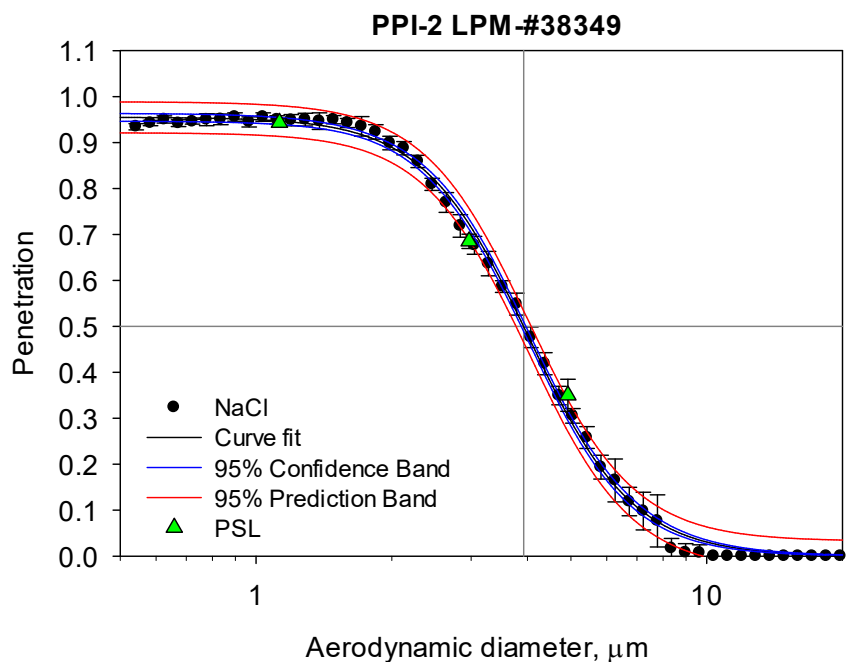


Figure 2. SKC 2-L/min-PPI impactor penetration curve as a function of particle size: a) individual data points and b) average values and standard deviations for each particle size and type based on six tests.

The data were fitted with a 3 parameter sigmoid regression equation resulting in the following equation:

$$\text{With NaCl: } \eta = \frac{0.9551}{1 + \left(\frac{dp}{4.021}\right)^{3.736}} \quad R^2=0.9985 \qquad \text{With PSL: } \eta = \frac{0.967}{1 + \left(\frac{dp}{4.041}\right)^{2.884}} \quad R^2=1 \qquad (2)$$

Based on the fit, the d_{50} cut size of the impactor was 3.92 μm with NaCl particles and 3.95 μm with PSL for the operating flow rate of 2 L/min.

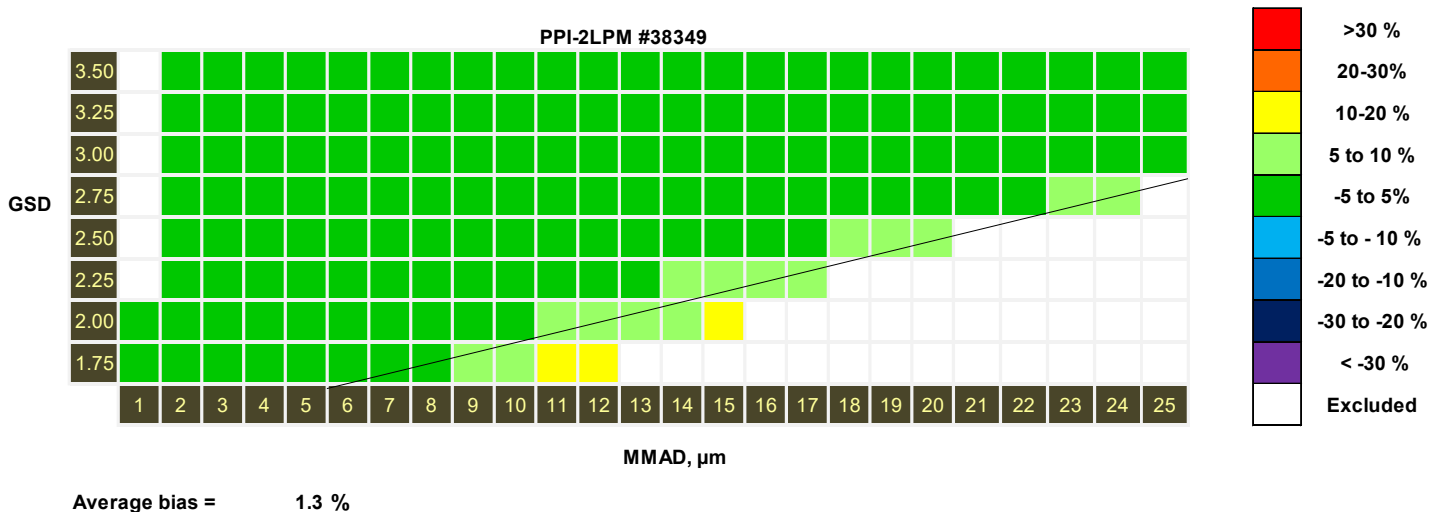


Figure 2c. Bias map for the SKC 2-L/min-PPI impactor (#38349) for different particle size distributions (MMAD and GSD).

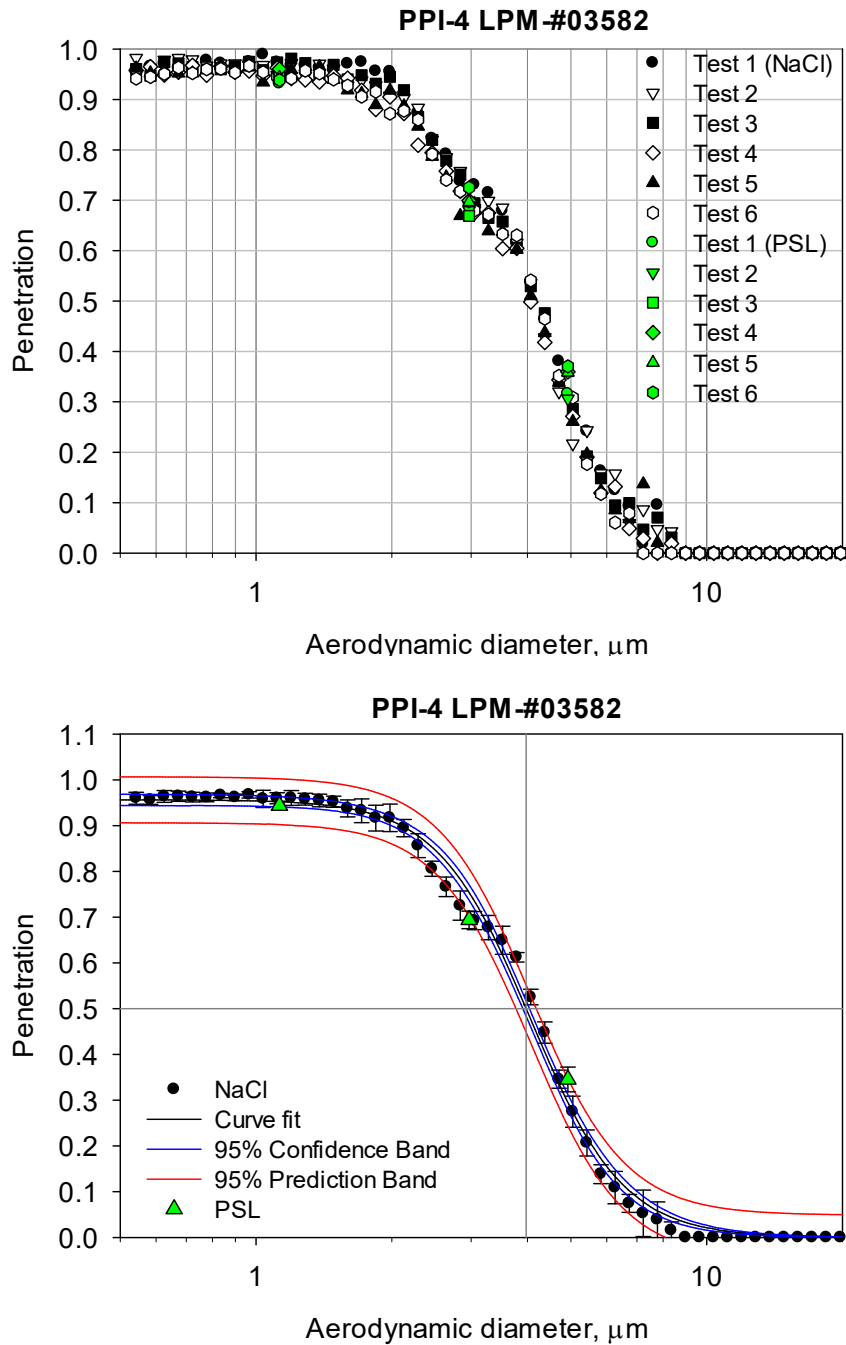


Figure 3. SKC 4-L/min-PPI impactor penetration curve as a function of particle size: a) individual data points and b) average values and standard deviations for each particle size and type based on six tests.

The data were fitted with a 3 parameter sigmoid regression equation resulting in the following equation:

$$\text{NaCl: } \eta = \frac{0.9569}{1 + \left(\frac{dp}{4.060}\right)^{4.176}} \quad R^2=0.9968 \quad \text{PSL: } \eta = \frac{0.9569}{1 + \left(\frac{dp}{4.060}\right)^{4.176}} \quad R^2=1 \quad (3)$$

Based on the fit, the d_{50} cut size of the impactor was 3.97 μm with NaCl and 3.96 μm with PSL for the operating flow rate of 4 L/min.

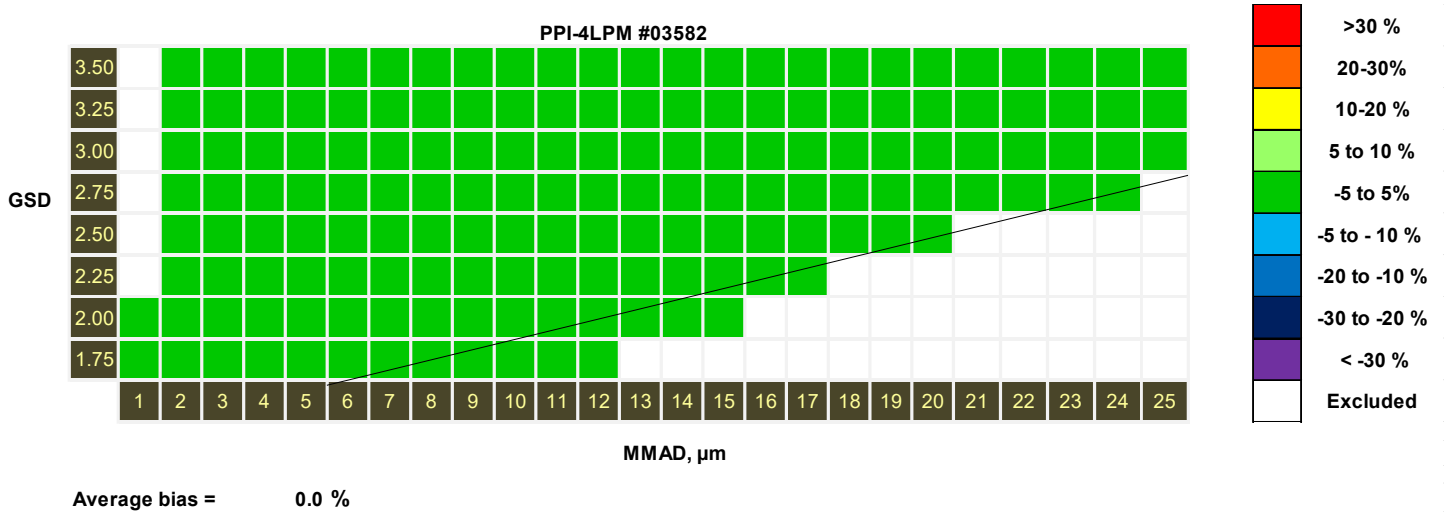


Figure 3c. Bias map for the 4-L/min-PPI impactor (#03582) for different particle size distributions (MMAD and GSD).

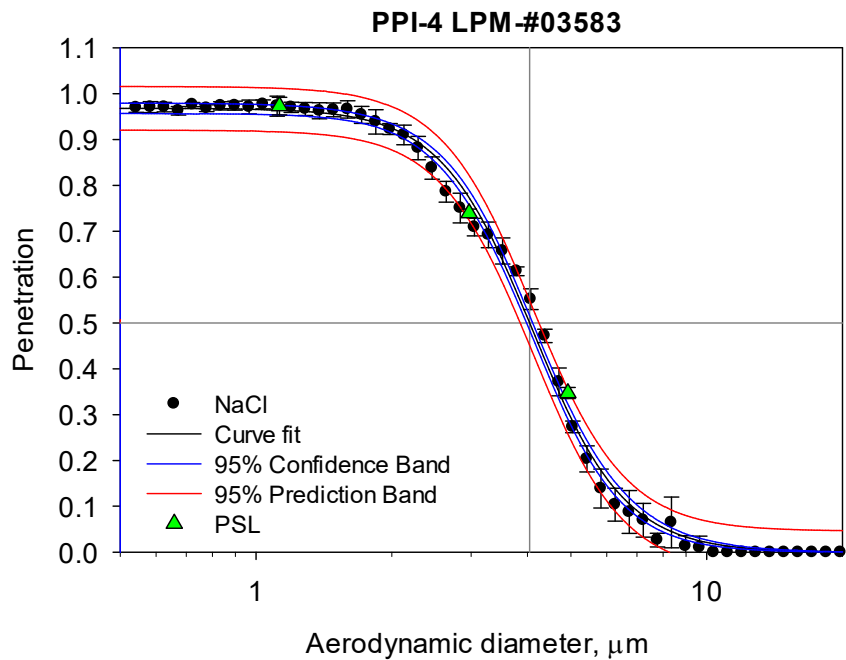
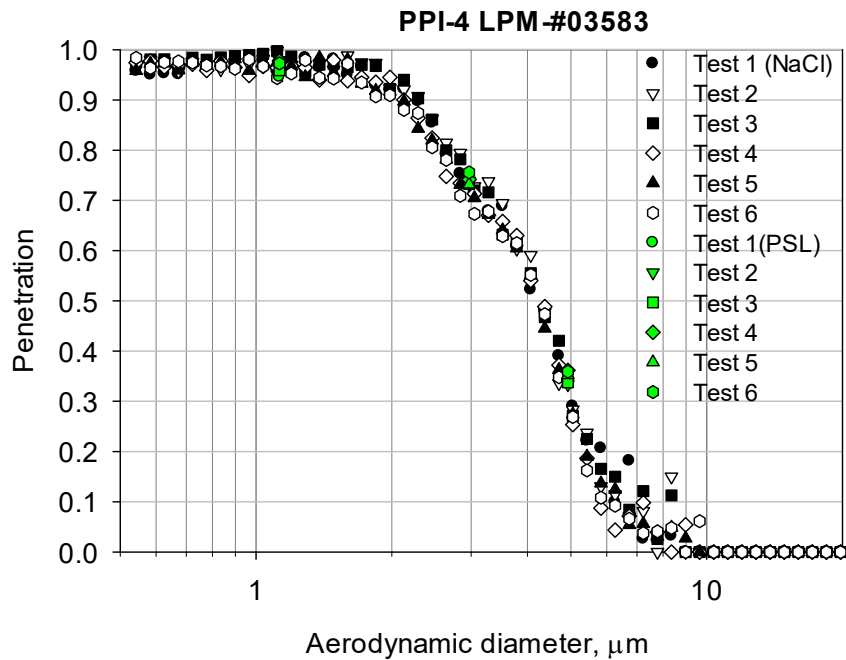


Figure 4. SKC 4-L/min-PPI impactor penetration curve as a function of particle size: a) individual data points and b) average values and standard deviations for each particle size and type based on six tests.

The data were fitted with a 3 parameter sigmoid regression equation resulting in the following equation:

$$\text{NaCl: } \eta = \frac{0.9681}{1 + \left(\frac{dp}{4.108}\right)^{4.249}} \quad R^2=0.9971 \quad \text{PSL: } \eta = \frac{0.9848}{1 + \left(\frac{dp}{4.113}\right)^{3.393}} \quad R^2=1 \quad (4)$$

Based on the fit, the d_{50} cut size of the impactor was 4.04 μm with NaCl and 4.08 μm with PSL for the operating flow rate of 4 L/min.

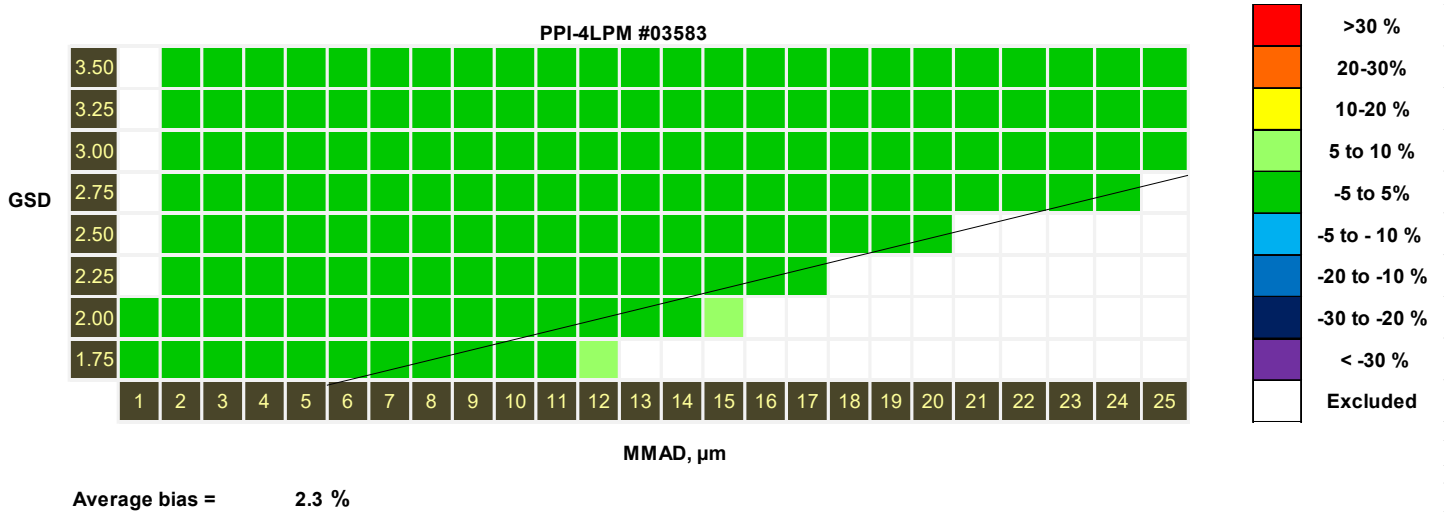


Figure 4c. Bias map for the SKC 4-L/min-PPI impactor (#03583) for different particle size distributions (MMAD and GSD).



(a)

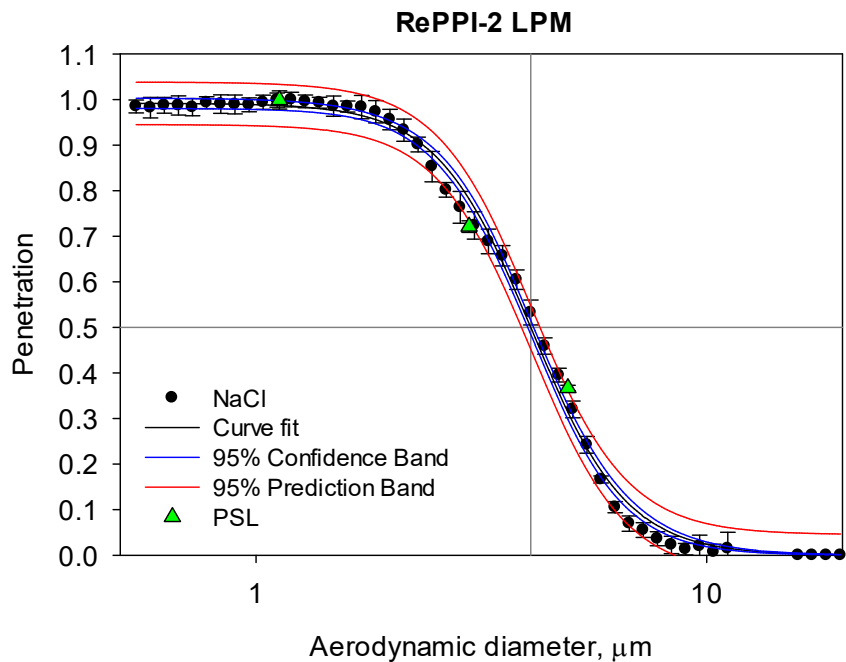
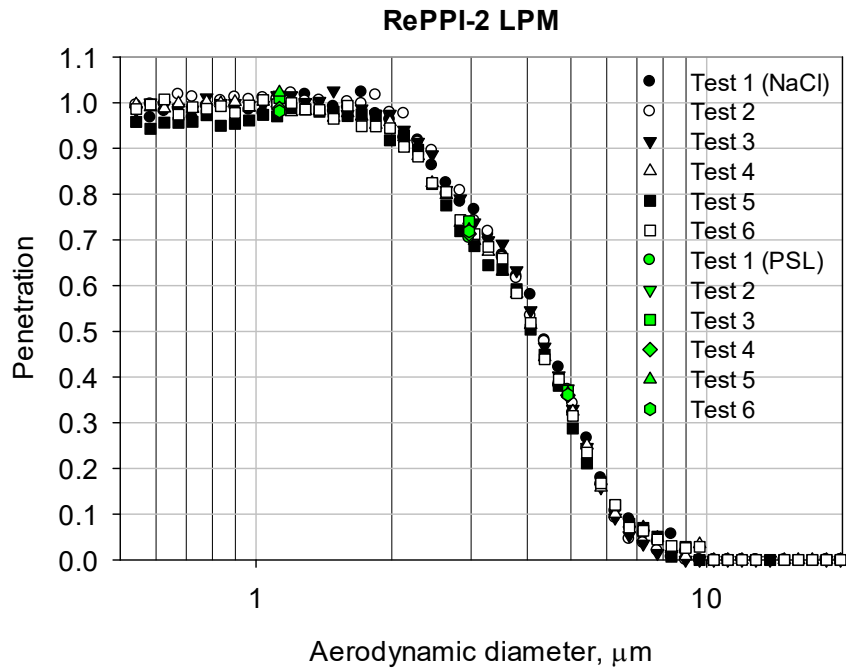


Figure 5. SKC 2-L/min-RePPI Impactor penetration curve as a function of particle size: a) individual data points and b) average values and standard deviations for each particle size and type based on six tests.

The data were fitted with a 3 parameter sigmoid regression equation resulting in the following equation:

$$\text{NaCl: } \eta = \frac{0.9918}{1 + \left(\frac{dp}{4.0841}\right)^{4.1274}} \quad R^2=0.9986 \quad \text{PSL: } \eta = \frac{1.025}{1 + \left(\frac{dp}{4.014}\right)^{2.871}} \quad R^2=1 \quad (5)$$

Based on the fit, the d_{50} cut size of the reusable impactor was $4.07 \mu\text{m}$ with NaCl and $4.08 \mu\text{m}$ with PSL for the operating flow rate of 2 L/min.

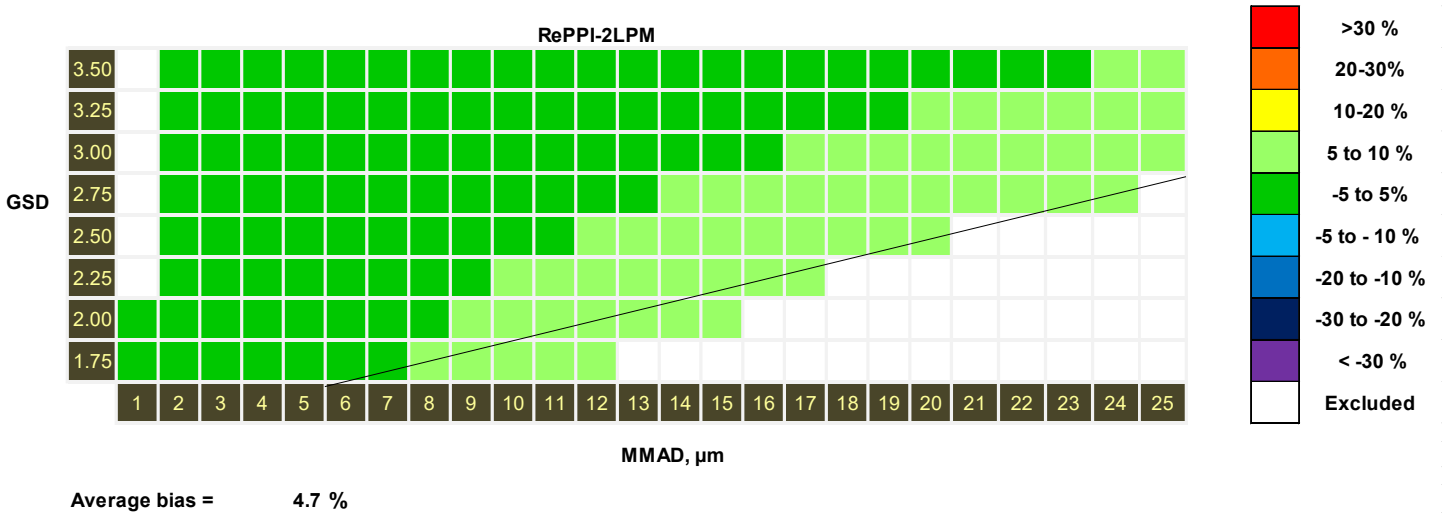


Figure 5c. Bias map for the SKC 2-L/min-RePPI Impactor for different particle size distributions (MMAD and GSD).

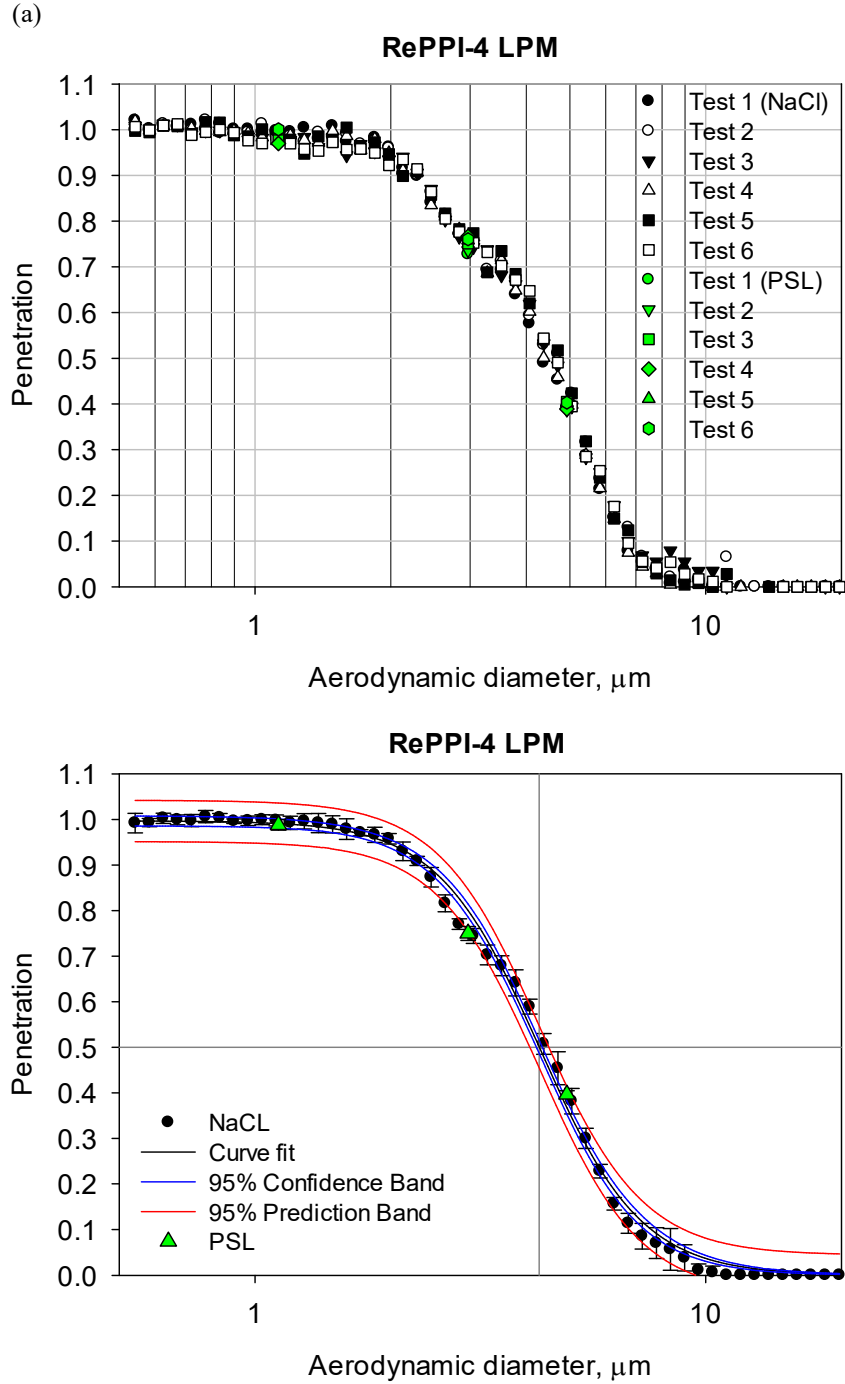


Figure 6. SKC 4-L/min-RePPI Impactor penetration curve as a function of particle size: a) individual data points and b) average values and standard deviations for each particle size and type based on six tests.

The data were fitted with a 3 parameter sigmoid regression equation resulting in the following equation:

$$\text{NaCl: } \eta = \frac{0.9969}{1 + \left(\frac{dp}{4.279}\right)^{3.8412}} \quad R^2=0.9975 \quad \text{PSL: } \eta = \frac{1.007}{1 + \left(\frac{dp}{4.256}\right)^{2.976}} \quad R^2=1 \quad (6)$$

Based on the fit, the d_{50} cut size of the reusable impactor was 4.27 μm with NaCl and 4.28 μm (with PSL) for the operating flow rate of 4 L/min.

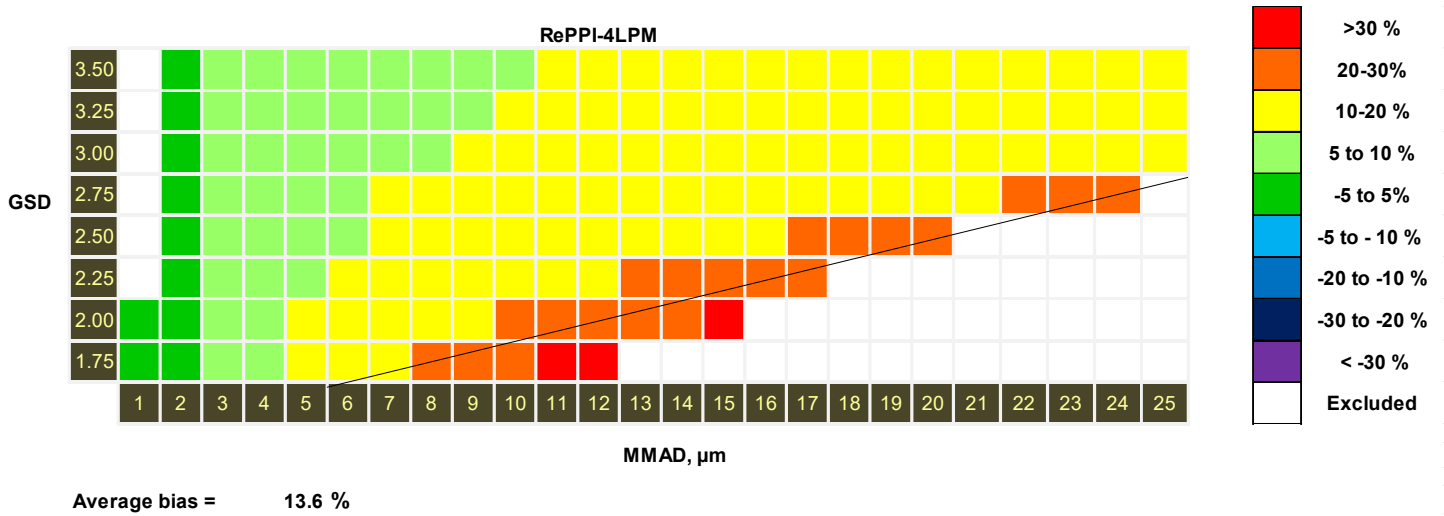


Figure 6c. Bias map for the SKC 4-L/min-RePPI Impactor for different particle size distributions (MMAD and GSD).



An additional test (2nd test) with 4-L/min-RePPI with sodium chloride

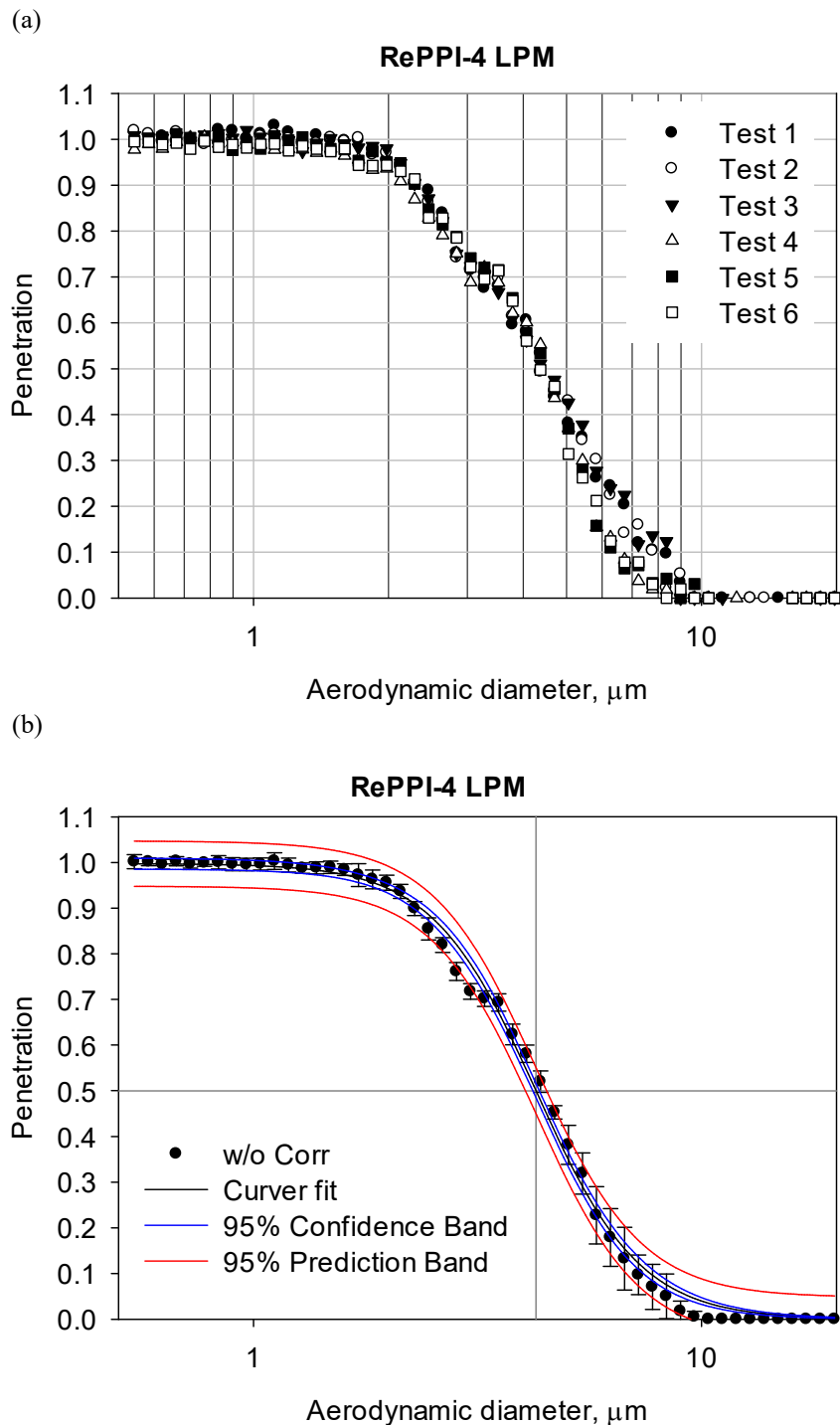


Figure 7. SKC 4-L/min-RePPI Impactor penetration curve as a function of particle size: a) individual data points and b) average values and standard deviations for each particle size and type based on six tests.



The data were fitted with a 3 parameter sigmoid regression equation resulting in the following equation:

$$\text{NaCl: } \eta = \frac{0.9976}{1 + \left(\frac{dp}{4.2755}\right)^{3.7369}} \quad R^2=0.9970 \quad (7)$$

Based on the fit, the d_{50} cut size (aerodynamic particle sizes at which 50% penetration occurs) of the impactor was 4.27 μm for the collection flow rate of 4 L/min.

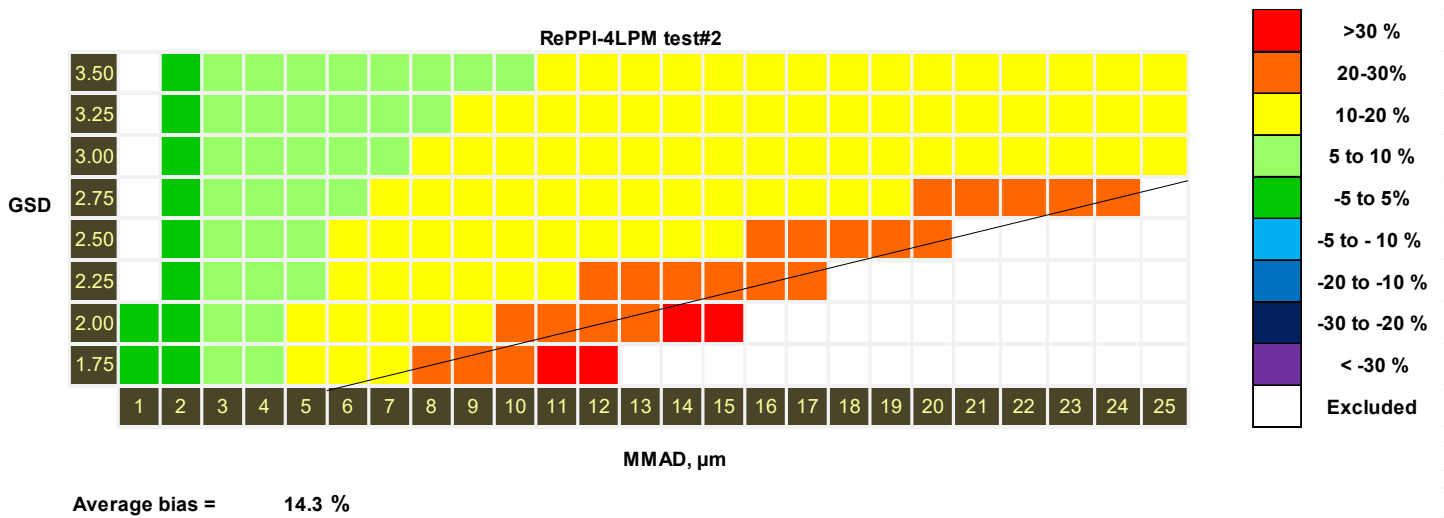


Figure 7c. Bias map for the SKC 4-L/min-RePPI Impactor for different particle size distributions (MMAD and GSD). Test #2 at 4 L/min.



An additional test of 4-L/min-RePPI at 4.3 L/min with sodium chloride particles

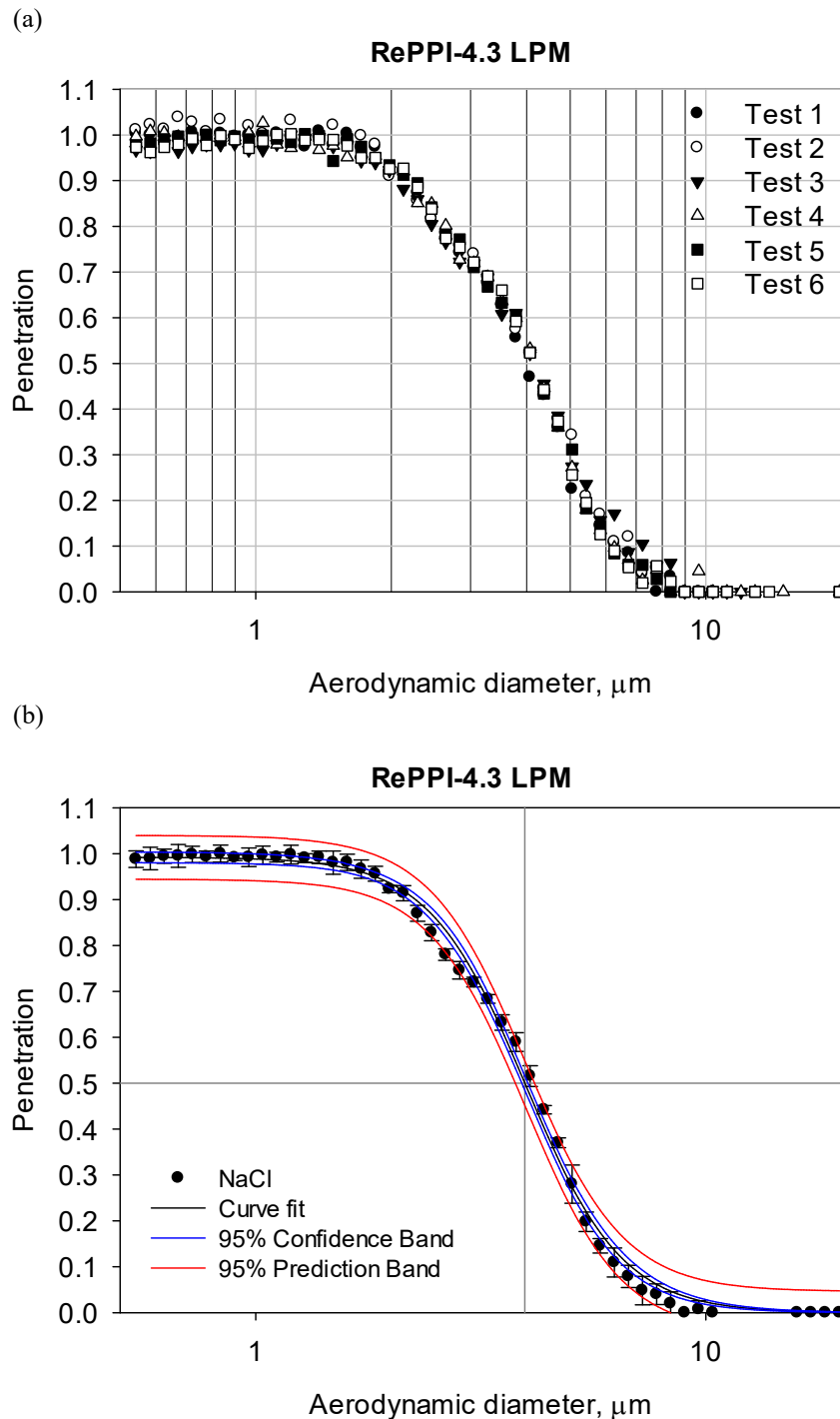


Figure 8. SKC 4-L/min-RePPI impactor penetration curve as a function of particle size when operated at 4.3 L/min: a) individual data points and b) average values and standard deviations for each particle size and type based on six tests.



The data were fitted with a 3 parameter sigmoid regression equation resulting in the following equation:

$$\text{NaCl: } \eta = \frac{0.9922}{1 + \left(\frac{dp}{3.977}\right)^{4.045}} \quad R^2=0.9971 \quad (8)$$

Based on the fit, the d_{50} cut size (aerodynamic particle sizes at which 50% penetration occurs) of the impactor was 3.96 μm for the collection flow rate of 4.3 L/min.

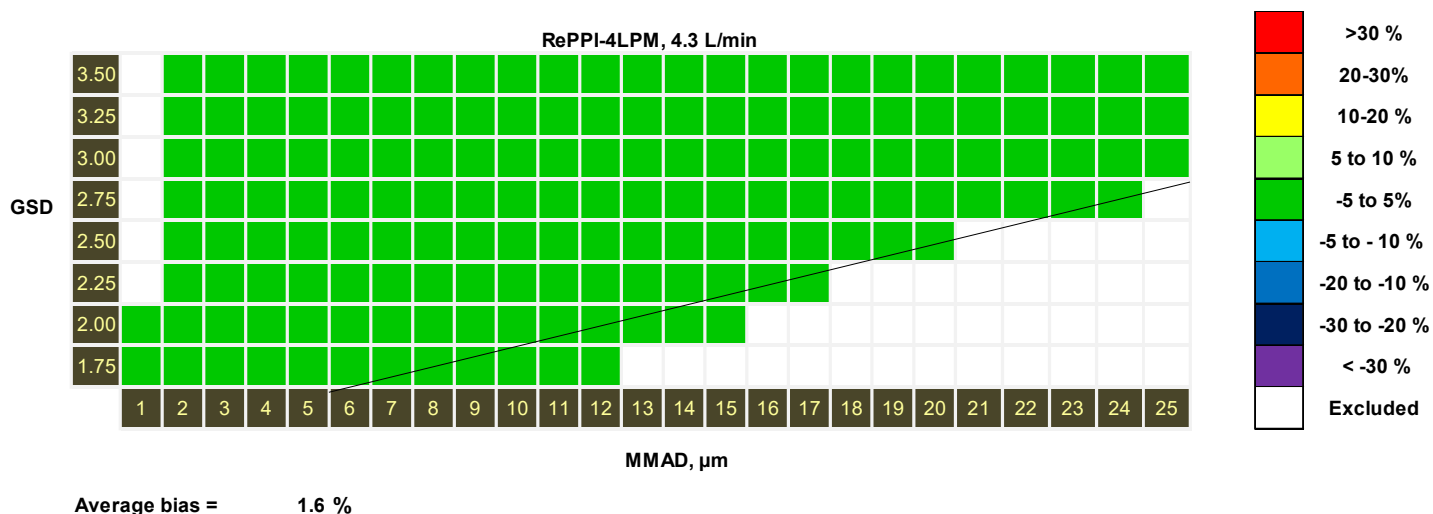


Figure 8c. Bias map for the SKC 4-L/min-RePPI Impactor operated at 4.3 L/min for different particle size distributions (MMAD and GSD).



An additional test with 4-L/min-RePPI impactor operated at 4.5 L/min and challenged with sodium chloride particles

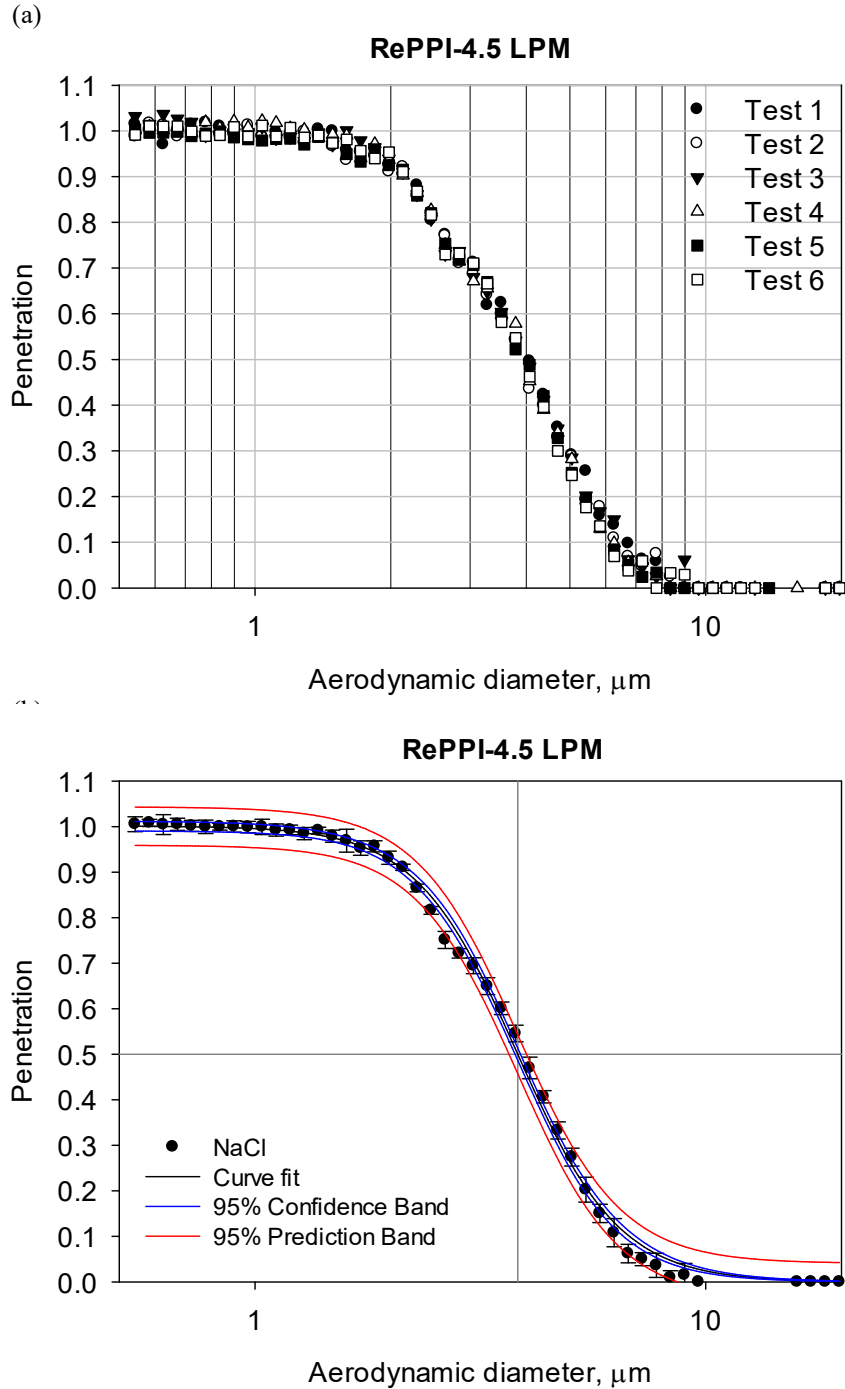


Figure 9. SKC RePPI-4.0 L/min impactor penetration curve as a function of particle size when tested at 4.5 L/min: a) individual data points and b) average values and standard deviations for each particle size.



The data were fitted with a 3 parameter sigmoid regression equation resulting in the following equation:

$$\text{NaCl: } \eta = \frac{1.001}{1 + \left(\frac{dp}{3.824}\right)^{3.843}} \quad R^2=0.9977 \quad (9)$$

Based on the fit, the d_{50} cut size (aerodynamic particle size at which 50% penetration occurs) of the impactor was 3.83 μm for collection flow rates of 4.5 L/min.

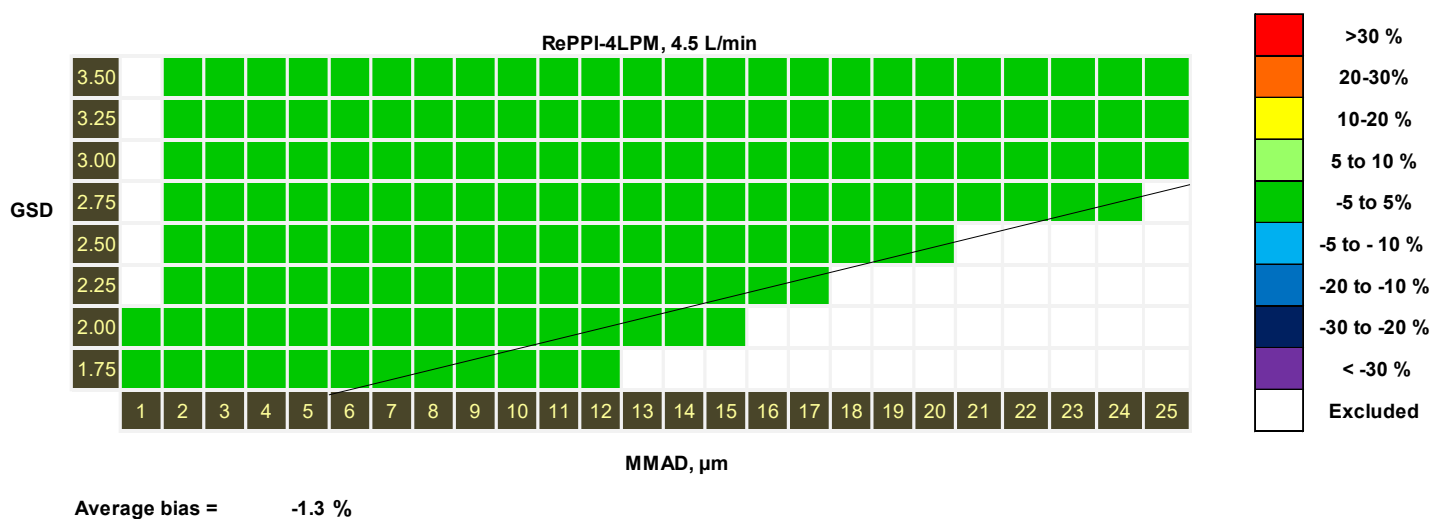


Figure 9c. Bias map for the SKC 4-L/min-RePPI Impactor operated at 4.3 L/min for different particle size distributions (MMAD and GSD).

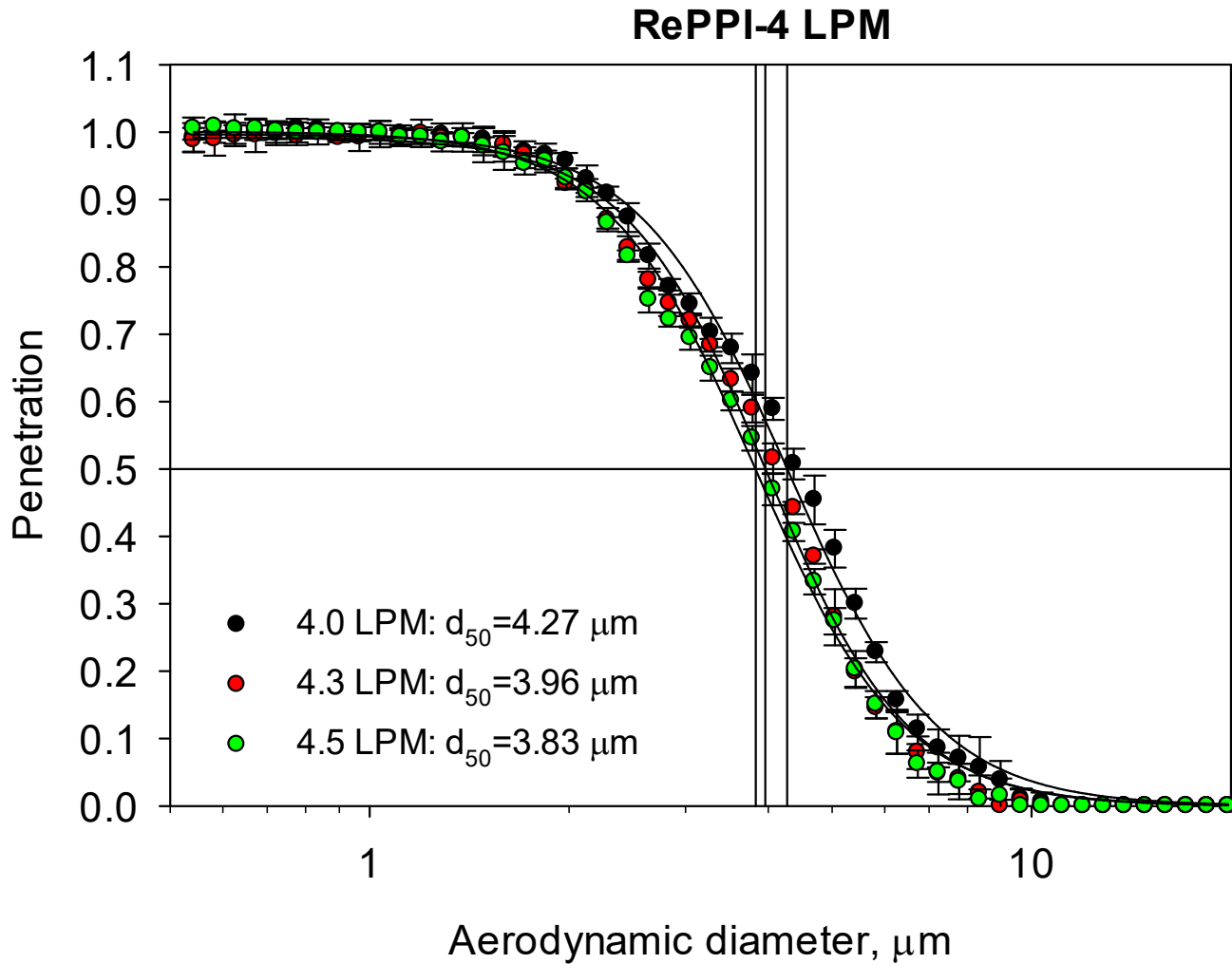


Figure 10. Comparison of RePPI – 4 L/min performance when operated at different flow rates.



An additional test of 4-L/min-PPI (#03582) with sodium chloride particles with PPI facing downward

(a)

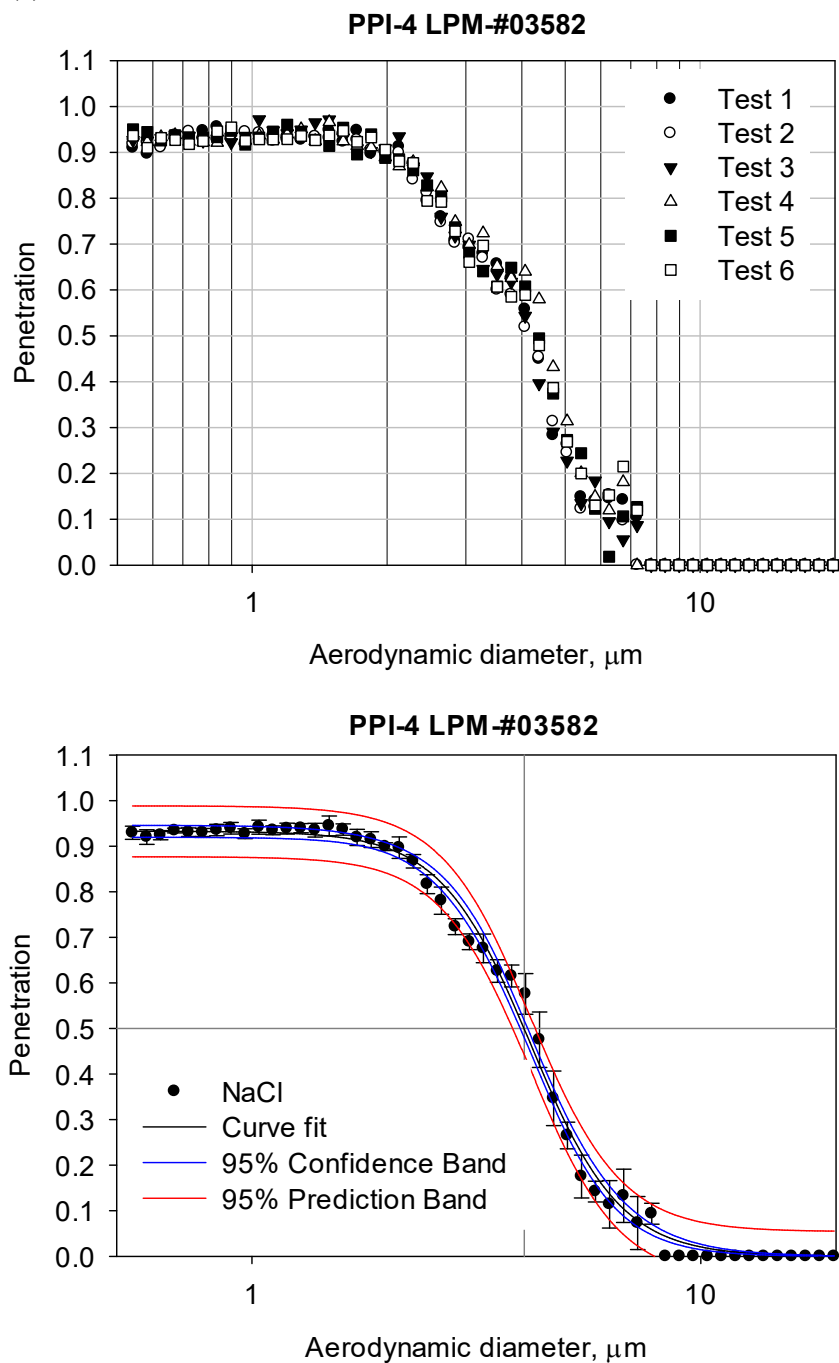


Figure 11. SKC 4-L/min-PPI Impactor penetration curve as a function of particle size: a) individual data point of the six tests and b) average of the six tests.



The data were fitted with a 3 parameter sigmoid regression equation resulting in the following equation:

$$\text{NaCl: } \eta = \frac{0.9328}{1 + \left(\frac{dp}{4.172}\right)^{4.335}} \quad R^2=0.9958 \quad (8)$$

Based on the fit, the d_{50} cut sizes of the impactor were 4.04 μm for collection flow rates of 4 L/min.

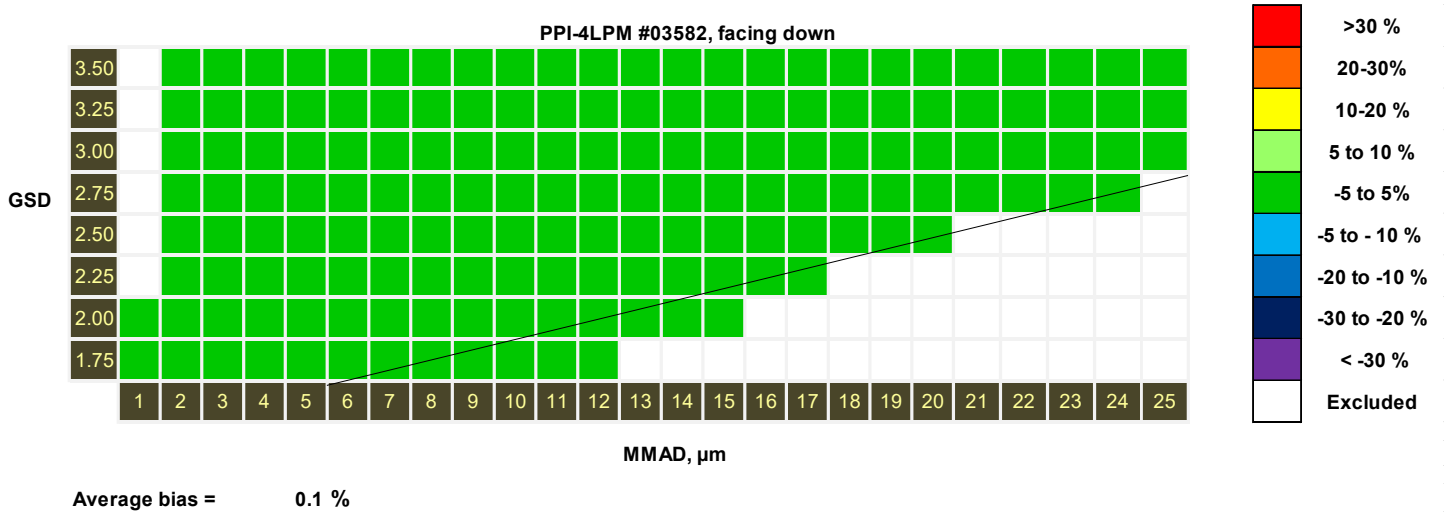


Figure 11c. Bias map for the SKC 4-L/min-PPI impactor (#03582) for different particle size distributions (MMAD and GSD) with the impactor oriented downward.



An additional test of 4-L/min-PPI (#03582) with sodium chloride particles with PPI oriented sideways

(a)

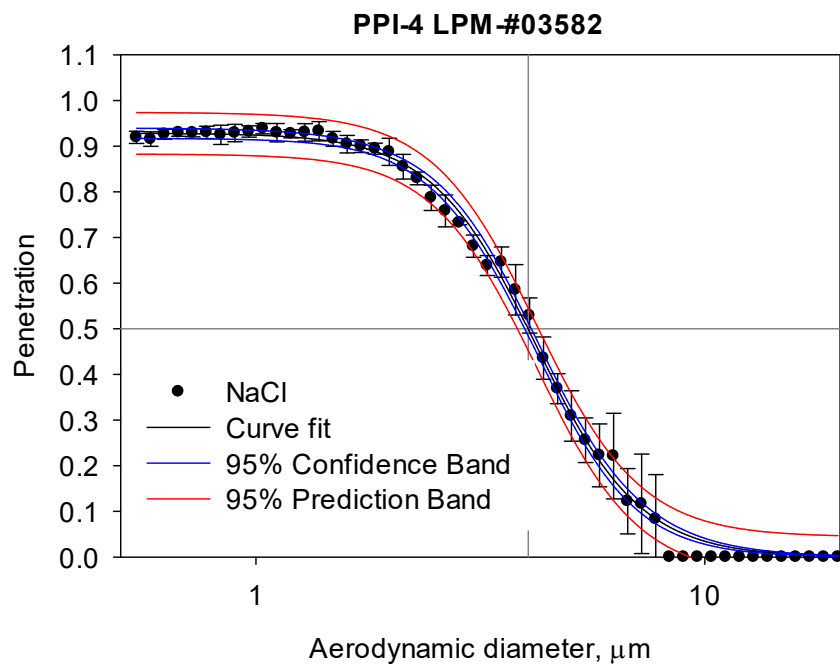
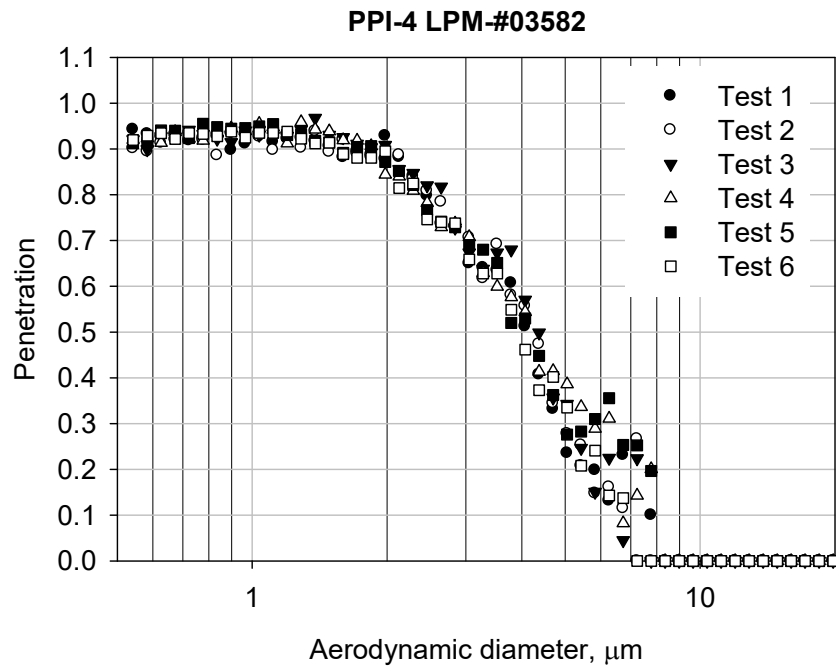


Figure 12. SKC 4-L/min-PPI Impactor penetration curve as a function of particle size: a) individual data point of the six tests and b) average of the six tests.

The data were fitted with a 3 parameter sigmoid regression equation resulting in the following equation:



$$\text{NaCl: } \eta = \frac{0.9284}{1 + \left(\frac{dp}{4.205}\right)^{3.754}} \quad R^2=0.9970 \quad (9)$$

Based on the fit, the d_{50} cut sizes of the impactor were 4.04 μm for collection flow rates of 4 L/min.

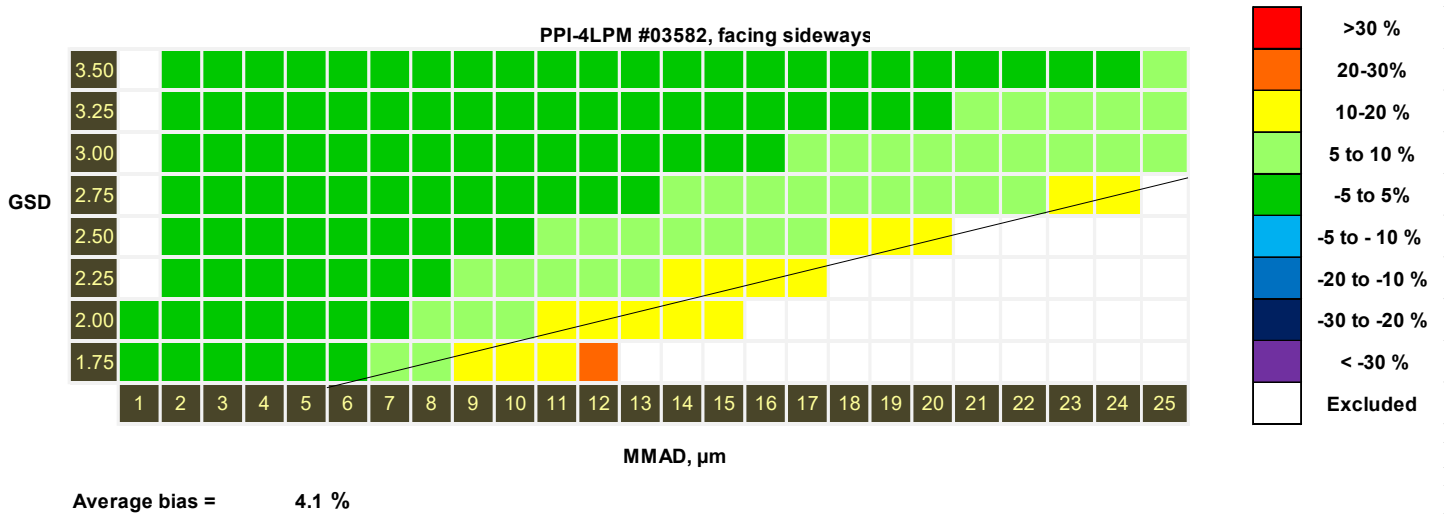


Figure 12c. Bias map for the SKC 4-L/min-PPI impactor (#03582) for different particle size distributions (MMAD and GSD) with the impactor oriented sideways.



Summary of Penetration Efficiency Results

Penetration efficiency

The tested SKC 2-L/min-PPI, 4-L/min-PPI, and SKC 2-L/min-RePPI showed cut-off sizes very close to the expected and theoretically predicted value of 4.0 μm .

The tested 4-L/min-PPI (#03582) showed tolerance to its orientation, and its d_{50} was close to 4.0 μm when the sampler was oriented both downward and sideways.

The d_{50} for the SKC 4-L/min-RePPI was higher at 4.27 μm . This result was confirmed in an additional set of measurements. Extra sets of measurements showed that the d_{50} could be brought to the expected range with a slightly increased sampling flow rate of 4.3 L/min, i.e., less than 10 % flowrate increase. The reasons for higher d_{50} of the SKC 4-L/min-Re PPI are unknown at this point. It is suggested that the manufacturer analyzes the structure and physical dimensions of the SKC 4-L/min-Re PPI for deviations from the specifications. If such variations are found and confirmed, the impactor design should be adjusted, and the impactor retested.

Bias maps

A similar pattern was observed for the bias maps: bias maps for the tested SKC 2-L/min-PPI, 4-L/min-PPI, and SKC 2-L/min-RePPI showed little deviation from the expected performance, and for the vast majority of challenge aerosol, the bias was within +/-5%. The average bias for the two SKC 2-L/min-PPI units was 1.3% and 1.7%. The two SKC 4-L/min-PPI units showed an average bias of 0.0% and 2.3%. The SKC 2-L/min-RePPI showed the average bias of 4.7%.

The average bias for SKC 4-L/min-RePPI was 13.6% and 14.3% in the two tests when the impactor was operated at a nominal 4 L/min flowrate. However, the average bias decreased to 1.6% and -1.3% when the sampling flow rate was increased to 4.3 and 4.5 L/min, respectively.

The tested 4-L/min-PPI (#03582) showed tolerance to its orientation: with the sampler oriented downward, the average bias was 0.1%, and when the sampler was oriented sideways, the average bias became 4.1%.

For all tested samplers, the strongest biases occurred when challenged with the aerosol that had large MMAD and relatively low GSD.



RUTGERS

School of Environmental
and Biological Sciences

BIOAEROSOL RESEARCH AND TECHNOLOGY

References

1. American Society for Testing Materials. Standard Practice for Evaluating the Performance of Respirable Aerosol Samplers (D6061 - 01). 2012.